



Elevated ATF4 Expression in Odontogenic Keratocysts Epithelia: Potential Involvement in Tissue Hypoxia and Stromal M2 Macrophage Infiltration

Wen-Qun Zhong*, Zhi-Zheng Li*, Hao Jiang, Yan-Ping Zou, Hai-Tao Wang, Yu Cai, Yi Zhao, and Ji-Hong Zhao

State Key Laboratory Breeding Base of Basic Science of Stomatology (Hubei-MOST) & Key Laboratory of Oral Biomedicine Ministry of Education, School & Hospital of Stomatology (W-QZ, Z-ZL, HJ, Y-PZ, H-TW, YC, YZ, J-HZ), Department of Oral and Maxillofacial Surgery, School & Hospital of Stomatology, (W-QZ, YC, J-HZ), and Department of Prosthodontics, School & Hospital of Stomatology (YZ), Wuhan University, Wuhan, China

Summary

The aim of this study was to investigate the expression of the activating transcription factor 4 (ATF4) in odontogenic keratocysts (OKC), its association with hypoxia and M2-polarized macrophages infiltration, and its potential relationships with angiogenesis in OKC. The expression of ATF4, hypoxia-inducible factor 1 α (HIF-1 α), macrophage colony-stimulating factor (M-CSF), and receptor activator of nuclear factor κ -B ligand (RANKL) in OKC samples and normal oral mucosa (OM) was detected by immunohistochemistry. Meanwhile, microvessel density (MVD) was measured using antibody against CD31. M2-polarized macrophages were identified using double-staining for CD68⁺ and CD163⁺. The correlations of ATF4 with HIF-1 α , M-CSF, and M2-polarized macrophages infiltration were determined by Spearman's rank correlation test and hierarchical clustering. Human immortalized oral epithelial cells (HIOECs) were used in *in vitro* experiments. Our data showed that the expression of HIF-1 α , ATF4, and M-CSF was significantly upregulated in the epithelium of OKC when compared with the OM. The expression of ATF4 was positively correlated with that of HIF-1 α , M-CSF, MVD, and M2-polarized macrophages infiltration. Elevated expression of ATF4 in the epithelial lining of OKC may facilitate the M2 macrophages infiltration in response to hypoxia, leading to the development of OKC. (J Histochem Cytochem 67: 801–812, 2019)

Keywords

activating transcription factor 4, hypoxia, M2-polarized macrophages, odontogenic keratocysts

Introduction

Odontogenic keratocysts (OKC) are one of the most common cysts of jaw.¹ Recent studies indicated that not only epithelial lining but also the stromal components of OKC could promote vital processes, including lesion growth, invasion, and angiogenesis.^{1–3} In view of its aggressive behavior, including invasive growth and postoperative recurrence, further studies are needed to fully understand the mechanisms involved in progression of this disease.⁴

Activating transcription factor 4 (ATF4) is a member of the CREB (cAMP-response element binding protein) family with plenty of dimerization partners. It serves as

Received for publication February 7, 2019; accepted July 29, 2019.

*These authors contributed equally to this article.

Corresponding Authors:

Yi Zhao, State Key Laboratory Breeding Base of Basic Science of Stomatology (Hubei-MOST) & Key Laboratory of Oral Biomedicine Ministry of Education, School & Hospital of Stomatology, Wuhan University, No. 237 Luoyu Road, Wuhan 430079, China.
E-mail: zhao_yi@whu.edu.cn

Ji-Hong Zhao, State Key Laboratory Breeding Base of Basic Science of Stomatology (Hubei-MOST) & Key Laboratory of Oral Biomedicine Ministry of Education, School & Hospital of Stomatology, Wuhan University, No. 237 Luoyu Road, Wuhan 430079, China.
E-mail: jhzhao988@whu.edu.cn

an intermediary regulator in response to internal signals or external stimulating factors, and then mediates the expression of several genes associated with the development of various diseases, including breast cancer, endometrial cancer, retinal complications of diabetes, lupus nephritis, and neurodegenerative diseases.^{5–8} For instance, ATF4 could upregulate the expression of macrophage colony-stimulating factor (M-CSF) in human gliomas, leading to M2-polarized macrophages infiltration.⁹ In rheumatoid arthritis, ATF4 has been shown to cooperate with C/EBP-LIP, promoting RANKL gene expression and osteoclast formation in the synovium, thus contributing to disease progression.¹⁰ On the contrary, stress signals, including hypoxia, amino acid deprivation, oxidative stress, and endoplasmic reticulum stress (ERS), can act on ATF4 and enhance its expression.¹¹ For example, in breast cancer, hypoxic condition affects protein foldability in endoplasmic reticulum (ER), leading to the overexpression of ATF4. Furthermore, overexpressed ATF4 facilitates many tumor-related genes expression, including LAMP3 and JNK, and finally contributes to the growth and migration of breast cancer.^{11–13}

Hypoxia, which occurs when oxygen demand exceeds supply, is one pivotal microenvironmental parameter historically implicated in tumor growth, invasion, and angiogenesis.^{14,15} Several reports have shown that hypoxia is closely related to vascular remodeling, and osteoclastogenesis in diseases such as osteoporosis, rheumatoid osteoarthritis, and wound healing.^{16–18} A number of recent researches have confirmed that the microenvironment of odontogenic cysts and tumors in jaw often became hypoxic, which may play crucial role in their development.^{19,20} Hypoxia-inducible factor-1 α (HIF-1 α) is considered to be a master regulator of the cellular response to hypoxia, and meanwhile serves as an objective index of cellular hypoxia-sensing mechanism.¹⁵ Although HIF-1 α was found to be upregulated in odontogenic lesions, the contribution of hypoxia to pathological changes of OKC is still not well understood.

Macrophages are essential components of the immune system in stroma and play an important role in the regulation of microenvironment.²¹ Under different stimulating factors, macrophages can be induced to differentiate into two polarization types: classical M1 and alternative M2-polarized macrophages. M2-polarized macrophages, also called tumor-associated macrophages (TAMs), express high levels of CD68 and CD163, contribute to angiogenesis and immunosuppression, and promote invasion and angiogenesis of tumors.²¹

M2-polarized macrophages can be induced by several factors, and M-CSF is one of the most classic

inducible factors that remarkably contributes to the infiltration and M2 polarization of macrophages.²² In addition, hypoxia as well contributes to the switches of macrophages into M2-polarized phenotype in tumors.²³ Although we have confirmed the infiltration of M2-polarized macrophages and their role in inducing angiogenesis of OKC in a previous study,¹ how the infiltration of M2 macrophages in OKC is modulated is still largely unclear.

In this study, the expression levels of ATF4, HIF-1 α , M-CSF, and RANKL in normal oral mucosa (OM) and OKC samples were detected by immunohistochemistry and the correlation between their expression levels was evaluated. The possible relationship between the expression levels of ATF4 and the infiltration of M2 macrophages and angiogenesis was also studied. We found that the expression of ATF4 was elevated and closely correlated with tissue hypoxia, M2-polarized macrophages infiltration, and angiogenesis in OKC.

Materials and Methods

Specimens

Thirty-five OKC samples and 17 normal OM samples were collected at the Hospital of Stomatology, Wuhan University (Wuhan, China). Diagnosis of each case was histologically confirmed by the Pathology Department of Hospital of Stomatology, Wuhan University, before any experimental procedures. Clinical features of 35 OKC patients involved in this research were shown in Table 1. This study was approved by the review board of the Ethics Committee of Hospital of Stomatology, Wuhan University. Meanwhile, the use of clinical tissues in this research was carried out according to the World Medical Association Declaration of Helsinki and the National Institutes of Health Guidelines. Written informed consent was obtained from all the volunteers of our study.

Immunohistochemistry

Immunohistochemistry was performed as our previous studies.³ Briefly, specimens were fixed in 4% paraformaldehyde for 2–3 days, embedded in paraffin, sliced into 4- μ m tissue sections, and dewaxed in xylene. The antigen retrieval was performed by high pressure. Afterward, the slices were incubated with 3% hydrogen peroxide at 37C for 20 min and blocked with goat serum for 20 min. Furthermore, primary antibodies, including HIF-1 α (1:200; Abcam, Cambridge, UK), ATF4 (1:300; Proteintech, Wuhan, China), M-CSF (1:200; Epitomics, Burlingame, CA), RANKL (1:200;

Table 1. Summary of Clinical Features of Odontogenic Keratocysts Patients.

Patient No.	Gender	Age (years)	Location	Therapy
1	F	34	Mandible	Curettage
2	M	44	Maxilla	Curettage
3	M	32	Mandible	Curettage
4	F	56	Mandible	Curettage
5	F	58	Mandible	Curettage
6	F	24	Mandible	Curettage
7	F	78	Mandible	Curettage
8	M	35	Maxilla	Curettage
9	F	66	Mandible	Curettage
10	M	17	Maxilla	Curettage
11	M	42	Mandible	Curettage
12	F	49	Mandible	Curettage
13	M	52	Maxilla	Curettage
14	F	64	Mandible	Curettage
15	M	22	Maxilla	Curettage
16	M	36	Mandible	Curettage
17	M	69	Mandible	Curettage
18	M	56	Maxilla	Curettage
19	F	18	Mandible	Curettage
20	F	42	Mandible	Curettage
21	F	48	Mandible	Curettage
22	F	56	Mandible	Curettage
23	M	25	Mandible	Curettage
24	M	65	Mandible	Curettage
25	F	22	Maxilla	Curettage
26	M	36	Mandible	Curettage
27	F	45	Mandible	Curettage
28	F	13	Mandible	Curettage
29	F	65	Mandible	Curettage
30	M	33	Mandible	Curettage
31	F	23	Mandible	Curettage
32	M	48	Mandible	Curettage
33	F	27	Maxilla	Curettage
34	M	19	Mandible	Curettage
35	M	54	Mandible	Curettage

Proteintech, Wuhan, China), CD31 (1:200; Epitomics, San Francisco, CA), were added to the sections and incubated overnight at 4°C. After incubated with secondary antibodies, the sections were immersed in diaminobenzidine for the antibody staining, with development for less than 5 min until the stable staining intensity was reached. The negative control slides were set by using PBS buffer instead of the primary antibodies. Positive controls were infantile hemangioma slides, which were known to have positive staining for ATF4, HIF-1 α , and M-CSF. Oral squamous cell carcinoma slides, which are known to have positive staining for RANKL, were also used as positive controls. MVD was determined by counting the number of vessels as our previous studies.¹

Double-labeling Immunofluorescence

The procedures of double-labeling immunofluorescence were performed as previous description.¹ The negative control was made by using PBS buffer instead of the primary antibodies. Positive controls were performed by using infantile hemangioma slides for these evaluations.

Cell Culture

Human immortalized oral epithelial cells (HIOECs) were cultured in serum-free defined Keratinocyte-SFM medium (Gibco, Grand Island, NY), containing 5 ng/mL human recombinant growth factor, 100 U/mL penicillin, and 100 μ g/mL streptomycin. The cells were

Table 2. Primer Sequences Used for Real-time PCR.

Gene	Forward (5'-3')	Reverse (5'-3')
GAPDH	CGGAGTCAACGGATTTGGTCGTAT	AGCCTTCTCCATGGTGGTGAAGAC
HIF-1 α	ATCCATGTGACCATGAGGAAATG	TCGGCTAGTTAGGGTACACTTC
ATF4	CTCCGGGACAGATTGGATGTT	GGCTGCTTATTAGTCTCCTGGAC
M-CSF	AGACCTCGTGCCAAATTACATT	AGGTGTCTCATAGAAAGTTCGGA

Abbreviations: PCR, polymerase chain reaction; GAPDH, glyceraldehyde 3-phosphate dehydrogenase; HIF-1 α , hypoxia-inducible factor-1 α ; ATF4, activating transcription factor 4; M-CSF, macrophage colony-stimulating factor.

grown at 37C in a humidified incubator in an atmosphere of 5% CO₂. When grown to 70% confluence, the cells were treated with different concentrations of oxygen for 48 hr (hypoxia: 5% O₂, 1% O₂, or normoxia: 21% O₂) in anoxomat chambers (Mart Microbiology, Lichtenvoorde, the Netherlands) and then were collected for total RNA or protein to analyze expressions of HIF-1 α , ATF4, and M-CSF, respectively.

Western Blot Analysis

For Western immunoblotting analysis, HIOECs were collected in 1 \times SDS-PAGE loading buffer, and 20 μ g of total protein of each sample was separated by SDS-PAGE and transferred onto polyvinylidene difluoride (PVDF) membrane at 400 mA for 1.5 hr. After transfer, the membrane was blocked with blocking solution (5% dried skimmed milk), and then incubated with the primary antibodies (ATF4 [1:800; Proteintech, Wuhan, China], HIF-1 α [1:1000; Abcam, Cambridge, UK]) at 4C overnight. The blot was then washed with TBST (10 mM Tris-HCl, 150 mM NaCl, 0.1% Tween 20) for three times and incubated with horseradish peroxidase-conjugated secondary antibody for 1 hr at room temperature. Immunoblots were visualized by the ECL Western blotting substrate (Pierce, Woburn, MA) and recorded by a scanner (Canon, Tokyo, Japan).

Real-time Quantitative PCR

Total RNA was extracted and reversal transcribed to cDNA, using the E.Z.N.A. Total RNA Kit (Omega Bio-Tek, Norcross, GA) and the First-Strand cDNA Synthesis kit (Thermo Fisher, Waltham, PA), the procedures were followed as the manufacturer's protocol. After that, obtained cDNA was amplified in the standard conditions with the Fast Start Universal SYBR Green Master (Roche, Basel, Switzerland) on a Quant Studio 6 Flex Real-Time PCR System (Applied Biosystems, Carlsbad, CA), and glyceraldehyde-3-phosphate dehydrogenase (GAPDH) was selected as internal control. All the primer nucleotide sequences for real-time PCR were shown in Table 2.

Semi-quantitative Immunohistochemistry Analysis

Five random fields of each specimen were picked up by using a light microscope (Leica, Wetzlar, Germany) under a magnification of 200 \times . The immunohistochemistry scores were analyzed by the Image-Pro Plus version 6.0 software. Only epitheliums of each field were taken into account. Briefly, we used the "count/size" command to conduct a cell number-counting program. The basic steps were performed as follows: (1) define the area of interest, (2) set the reference value that identifies the positive staining, and (3) use the "pathology" command to count the objects automatically. Sum integrated optical density (IOD) and sum area (area) were generated from each specimen, and the quantitation was expressed as mean optical density (IOD/area) as our previous studies.³ For HIF-1 α , the staining was localized within both the cytoplasm and/or nucleus, but only the nuclear location was categorized as positive for HIF-1 α , which was expressed as the percentage of nuclear localization as previous studies.²⁴

Hierarchical Clustering and Statistical Analysis

As our previous description,²⁵ the immunohistochemical scores of each index were converted into scaled values centered on zero. The clustering analysis was conducted with Cluster 3.0 and the results were finally visualized with Java TreeView 1.0.5. Experiments were repeated three times at least before statistical analysis. Statistical analysis was performed with GraphPad Prism 5.03. Statistical analysis was done by Student's *t*-test and Spearman's rank correlation test; *p*<0.05 was considered significantly different.

Results

Overexpression of ATF4 in OKC Samples and Its Correlation With Hypoxia

To evaluate the expression level of ATF4 in OKC, immunohistochemistry was performed to assess the

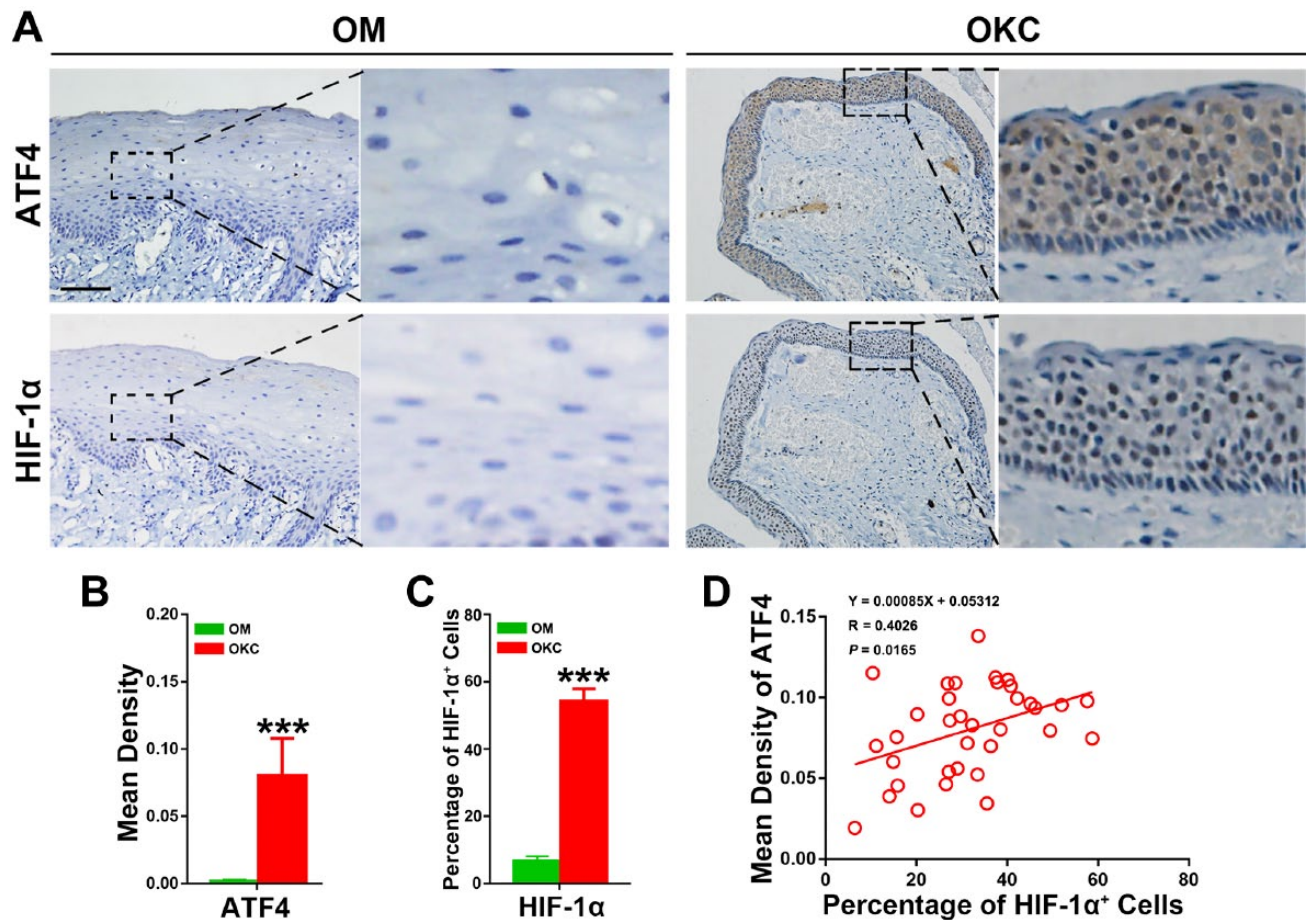


Figure 1. Expression levels of ATF4 and HIF-1 α in odontogenic keratocysts (OKC) and oral mucosa (OM) epithelium, and correlation test for the quantification of ATF4 and HIF-1 α proteins in OKC samples. (A) Increased expression of ATF4 and HIF-1 α was observed in OKC samples compared with OM samples. (B) Quantification of ATF4 and HIF-1 α expression levels in OKC and OM samples. (C) Quantification of HIF-1 α expression levels in OKC and OM samples. (D) Spearman's rank correlation analyses showed a positive correlation between ATF4 and HIF-1 α in OKC samples. Scale bar in (A) indicates 50 μ m. Abbreviations: ATF4, activating transcription factor 4; HIF-1 α , hypoxia-inducible factor 1 α . *** $p < 0.001$.

expression of ATF4 in 35 OKC and 17 OM samples. All 35 OKC samples expressed HIF-1 α and ATF4, although differed in the staining distribution and intensity. The representative immunohistochemical results were shown in Fig. 1A. The positive staining of ATF4 exhibited as dense distribution of brown granule in cytoplasm throughout the epithelium, including the basal, super layer cells, and a small amount brown nuclear staining in the epithelial cells. Contrary to OKC samples, the epithelium of OM samples barely had positive ATF4 staining.

To explore the potential association of ATF4 expression with hypoxia in OKC, HIF-1 α was also detected in OKC samples by immunohistochemistry. As shown in the Fig. 1A, positive immunoexpression of HIF-1 α represents as intense nuclear staining in both of the basal and super layer cells in the epithelium. By contrast, almost all OM samples presented HIF-1 α negatively

immunostaining. More importantly, Student's *t*-test further implicated that the expression levels of ATF4 ($p < 0.001$) and HIF-1 α ($p < 0.001$) were increased significantly in OKC relative to those in OM samples (Fig. 1B). To further explore the significance of HIF-1 α overexpression, the Spearman's rank correlation test was performed, and the results showed that ATF4 possessed a significant positive correlation with HIF-1 α (Fig. 1C). Collectively, these results revealed the activation of ATF4 and its possible association with the hypoxic microenvironment of OKC.

The M-CSF Expression in OKC and Its Close Association With ATF4

Then, we examined the immunoexpressions of M-CSF and RANKL in OKC and OM samples. As shown in

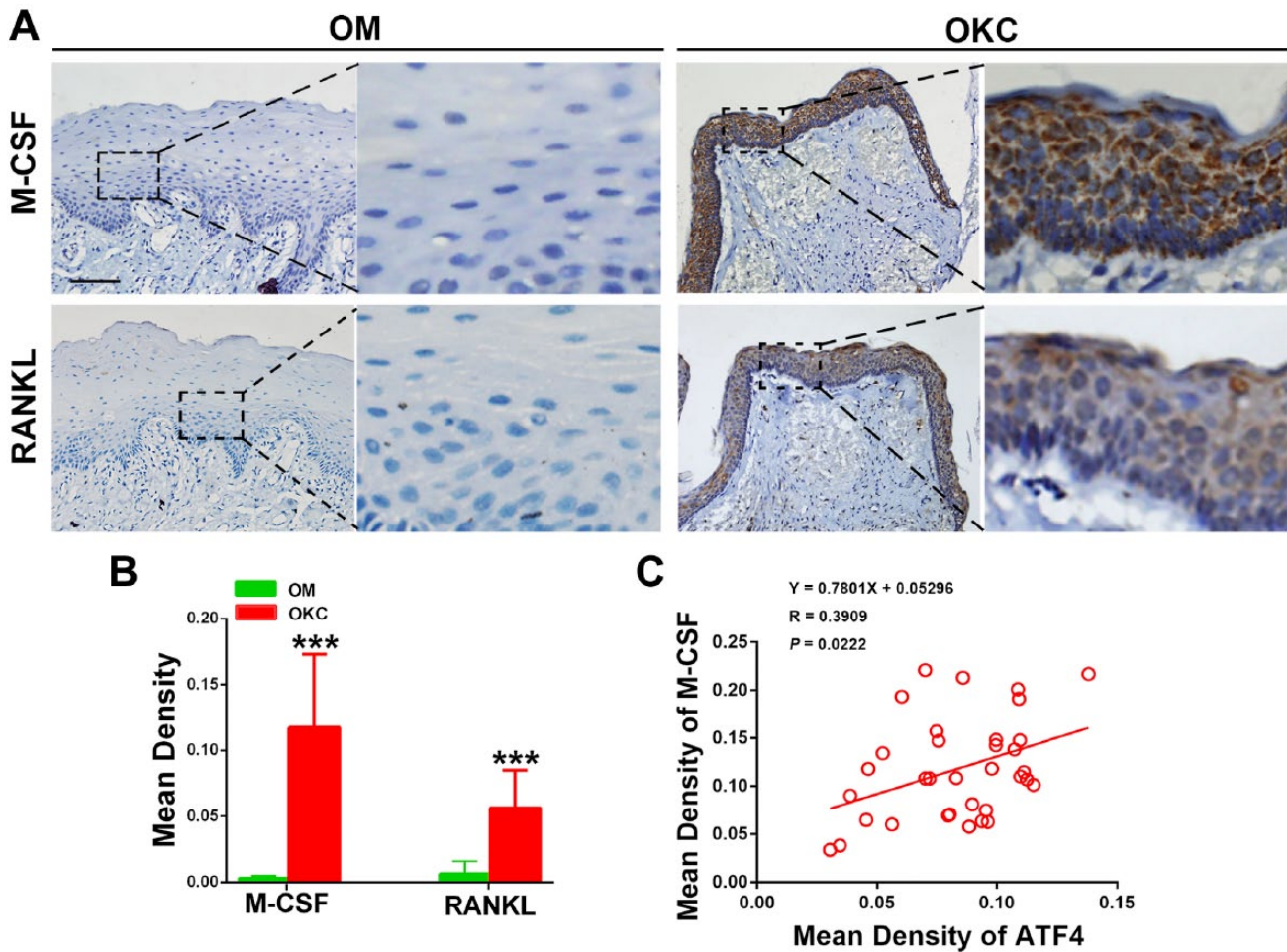


Figure 2. Expression levels of M-CSF and RANKL in odontogenic keratocysts (OKC) and oral mucosa (OM) epitheliums, and correlation test for the quantification of ATF4 and M-CSF in OKC samples. (A) Increased expression of M-CSF and RANKL was observed, compared with OM samples. (B) Quantification of M-CSF and RANKL expression levels in OKC and OM samples. (C) Correlation analysis showed a positive correlation with M-CSF and ATF4 in OKC samples. Scale bar in (A) indicates 50 μ m. Abbreviations: M-CSF, macrophage colony-stimulating factor; RANKL, receptor activator of nuclear factor κ -B ligand, ATF4, activating transcription factor 4. *** $p < 0.001$.

Fig. 2A, both of M-CSF and RANKL presented a strong staining in all layers of epithelium in OKC, but hardly any positive immunorexpression was observed in OM samples. Student's *t*-test further showed that the expression levels of M-CSF ($p < 0.001$) and RANKL ($p < 0.001$) were significantly increased in OKC compared with those in OM (Fig. 2B). To our interests, the result from immunochemical correlation analysis showed that ATF4 possessed a positive association with M-CSF (Fig. 2C) but not RANKL (Supplementary Material Fig. S1). These data suggested that M-CSF might participate in the function of ATF4 during the pathological development of OKC in the epithelium.

Synchronous Expression for ATF4 and M-CSF in OKC

To further validate the potential correlation between ATF4 and M-CSF, double-labeling immunofluorescence analyses for ATF4 and M-CSF were made on tissue samples from OKC and OM. As shown in Fig. 3, the strong staining of ATF4 was frequently observed in cytoplasm of epithelium in samples from OKC. Importantly, colocalization of ATF4 with the M-CSF signals was also been found in samples from OKC while immunofluorescent signals for ATF4 and M-CSF were nearly undetectable in the epithelium of tissue sample from OM.

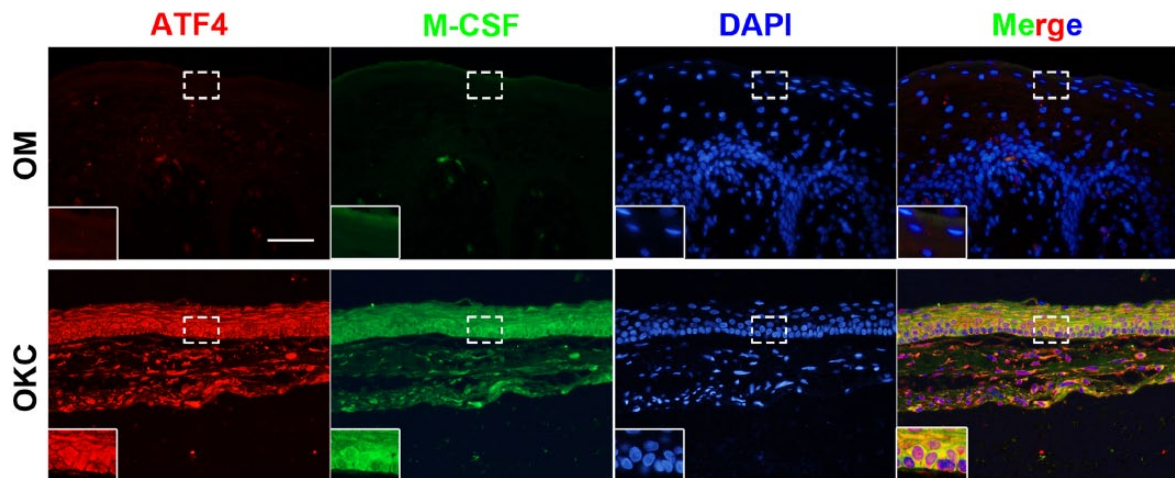


Figure 3. Double-labeling immunofluorescence staining for ATF4 and M-CSF in odontogenic keratocysts (OKC) and oral mucosa (OM) samples. As the magnified images indicated, the results showed a synchronous expression for ATF4 and M-CSF in both OKC and OM samples. Scale bar indicates 50 μm . Abbreviations: ATF4, activating transcription factor 4; M-CSF, macrophage colony-stimulating factor.

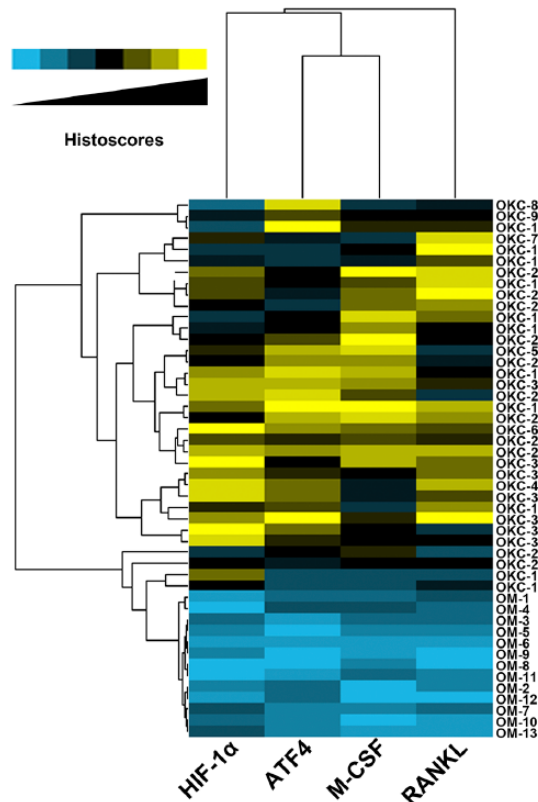


Figure 4. Hierarchical clustering analyses for the 35 odontogenic keratocysts (OKC) and 17 oral mucosa (OM) tissue samples. The relative relationship was directly shown by the length and subdivision of the branches in the heat map, the relative relationship between these tested proteins was showed on the top, and the relative relationship between these tissue samples was showed by the left. Abbreviations: HIF-1 α , hypoxia-inducible factor 1 α ; ATF4, activating transcription factor 4; M-CSF, macrophage colony-stimulating factor; RANKL, receptor activator of nuclear factor κ -B ligand.

Close Relation Between Markers Tested Reflected by the Cluster Analysis

To present our data more directly and nicely, the cluster analysis was performed and then visualized by using the heat map. As shown in Fig. 4, in the heat map, the correlations between cases (left) and tested markers (bottom) were reflected by the length and subdivision of the branches in the heat map. As expected, these proteins we tested were closely clustered (Fig. 4). The cluster analysis also verified the closest relation between ATF4 and HIF-1 α , which was in line with the results from the Spearman's correlation coefficient analysis. Meanwhile, almost all the OKC samples clustered together, which were distinguished from other cluster of OM samples. Taken together, the cluster analysis confirmed again the close relationships between the markers we tested.

ATF4 Were Positively Associated With the Infiltration of M2-polarized Macrophages and Angiogenesis in OKC

Double-labeling immunofluorescence of CD68⁺/CD163⁺ was used to determine M2-polarized macrophages as previous study.¹ As showed in Fig. 5, M2-polarized macrophages were frequently found in the stroma of OKC cyst wall tissues. In our present study, the ratio of CD68⁺/CD163⁺ (M2-polarized macrophages) in the total stromal cells ranged from 1.35% to 34.58%, with an average value of $20.70 \pm 8.04\%$. To explore the relationships between HIF-1 α , ATF4, M-CSF, and M2-polarized macrophages, Spearman's rank correlation tests and linear

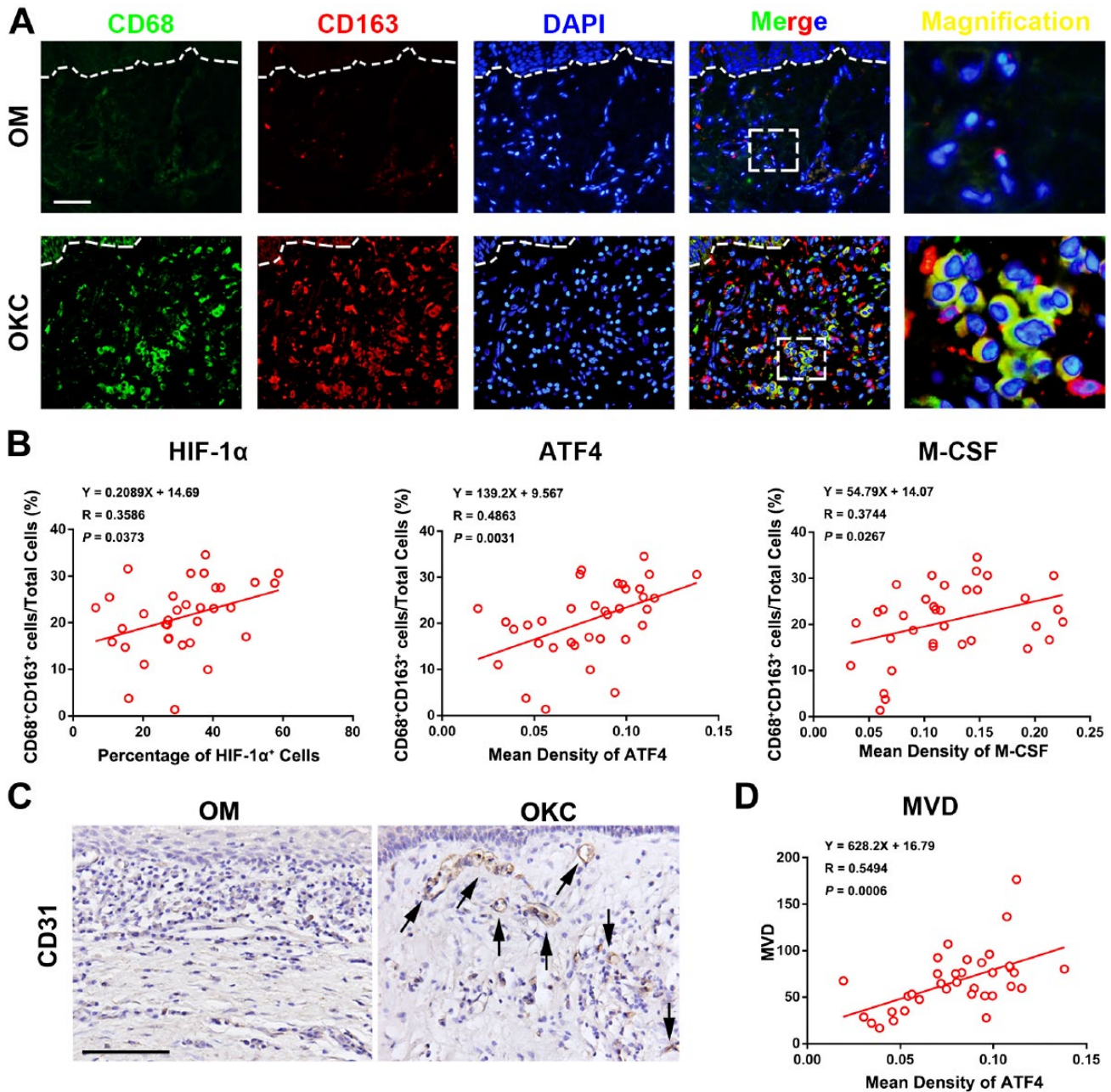


Figure 5. Correlation between ATF4 and M2-polarized macrophages as well as angiogenesis in odontogenic keratocysts (OKC) samples. (A) CD68⁺/CD163⁺ M2-polarized macrophages were detected in the stroma of OKC samples. (B) Correlation analyses showed a positive correlation with the percentage of M2 macrophage and these proteins respectively in OKC samples. (C) Staining of blood vessels with anti-CD31 antibody in OKC and OM samples. (D) Spearman's rank correlation test and linear regression were performed to assess the correlation of MVD with the expression level of ATF4 in OKC samples. Scale bars in (A) and (C) indicate 50 μ m. Abbreviations: ATF4, activating transcription factor 4; OM, oral mucosa; MVD, microvessel density; HIF-1 α , hypoxia-inducible factor-1 α ; M-CSF, macrophage colony-stimulating factor.

regression analyses were performed. The results showed that there were positive correlations between the appearance of M2-polarized macrophages and the expression of HIF-1 α , ATF4, and M-CSF, respectively.

Recent studies have documented that M2-polarized macrophages plays a central role in tumor angiogenesis while angiogenesis significantly contributes to the rapid growth of OKC.^{1,21,22} Therefore, we initially assessed the level of MVD in OKC by using anti-CD31

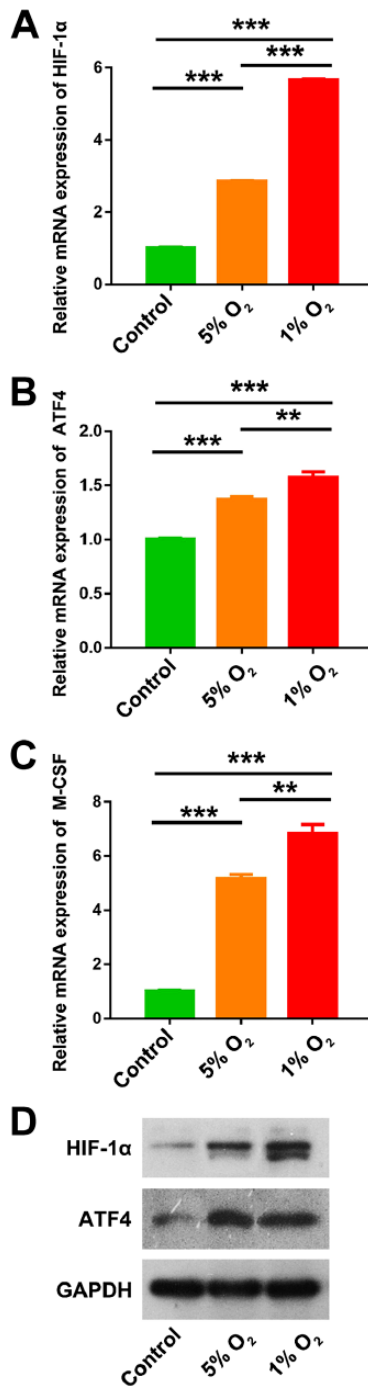


Figure 6. Induced expressions of HIF-1 α , ATF4, and M-CSF by hypoxia in human immortalized oral epithelial cells (HIOECs) in vitro. (A-C) Hypoxia (5% O₂, 1% O₂) significantly upregulated the mRNA expressions of HIF-1 α , ATF4, and M-CSF in HIOECs, compared with normal O₂ concentration (21% O₂) in vitro. (D) Hypoxia (5% O₂) significantly upregulated the expressions of HIF-1 α and ATF4, compared with normal O₂ concentration (21% O₂) in vitro. Abbreviations: HIF-1 α , hypoxia-inducible factor 1 α ; ATF4, activating transcription factor 4; M-CSF, macrophage colony-stimulating factor; GAPDH, glyceraldehyde-3-phosphate dehydrogenase. ** p <0.01. *** p <0.001.

antibody. As shown in Fig. 5C, CD31-positive vessels were primarily distributed in the stroma adjacent to the cystic epithelium lining and invasive front, which was in line with previous studies.¹ MVD was obviously higher in OKC than that in OM (Supplementary Material Fig. 2). To verify the potential significance of ATF4 in angiogenesis in OKC, we investigated the correlations between MVD and the expression of ATF4 in OKC by using Spearman's rank correlation tests. Intriguingly, the results showed that the expression level of ATF4 was significantly correlative with MVD in OKC samples. Collectively, these results implied that expression of ATF4 was closely associated with the presence of M2-polarized macrophages and angiogenesis in OKC.

Elevated Expressions of ATF4 and M-CSF Induced by Hypoxia in HIOECs In Vitro

HIOECs were cultured in hypoxia (5% O₂, 1% O₂) or normoxia (21% O₂) for 48 hr and a series of in vitro studies were performed. As shown in Fig. 6, the data from qPCR demonstrated that the mRNA levels of HIF-1 α , ATF4, and M-CSF were significantly upregulated under hypoxia condition in a dose-dependent way. Similarly, the results from Western blot confirmed that hypoxia obviously upregulated the expression of ATF4 in a dose-dependent way (Fig. 6D). These results confirmed that hypoxia could enhance the expressions of ATF4 and M-CSF in epithelial cells.

Discussion

Hypoxic microenvironment has been well documented to participate in many diseases through contributing to angiogenesis, lesions growth, and invasion.^{14,15}

In this study, we detected the expression level of HIF-1 α in OKC cyst wall tissues by immunohistochemistry. We found that the expression of HIF-1 α , the key marker of oxygen deprivation,¹⁵ was significantly increased in the epithelium of OKC, suggesting hypoxic status in the lesion of OKC. The hypoxic microenvironment in OKC epithelium may be caused by insufficient oxygen supply from underlying stroma and, at the same time, contribute to angiogenesis in underlying stroma. In this study, we found that microvessel density (MVD) of OKC was significantly increased compared with OM, although it did not alleviate the hypoxic condition in OKC epithelium. We suppose that this asymmetry between MVD and oxygen supply is closely related to the structure of underlying stroma. There are numerous stromal papillae running deeply into epithelium in OM, and the vascular loops walking

inside stromal papillae effectively supply the epithelium with oxygen.²⁶ Conversely, basal lamina of OKC cyst wall is completely straight, and the lack of stromal papillae and the vascular loops inside it could be the histological and architectural cause for the hypoxic microenvironment in OKC epithelium. Although hypoxic microenvironment widely exists in the lesions of OKC, the precise molecular mechanisms response to hypoxia remain largely unknown.

ATF4 is one of the stress responsive genes from ATF/CREB family. Under hypoxia, as the major transcriptional regulator in response to the Unfolded Protein Response (UPR), ATF4 can activate some genes to promote the restoration of ER function and survival of cells.^{12,14} In this study, we initially found the significant overexpression of ATF4 and its close correlation with hypoxia in the epithelial cells of OKC. Our present data implicated that ATF4 could be activated by oxygen deprivation and play a critical role in the cell adaptation to hypoxia. ATF4 might further regulate transcriptions of relative genes in OKC and then promote cell survival and lesion growth.

Basically, angiogenesis is necessary for oxygen and nutrients supply of rapid-expanded lesions. In tumors, M2-polarized macrophages play a crucial role in angiogenesis.²¹ Our previous studies have indicated that M2-polarized macrophages played a crucial role in controlling cyst angiogenesis by releasing various pro-angiogenic factors, including vascular endothelial growth factor (VEGF), transforming growth factor- β (TGF- β), and matrix metalloprotein-9 (MMP-9).¹ Notably, secreted by various cells, M-CSF is well known as the essential factor in the recruitment, differentiation, and polarization of M2-polarized macrophages.²² On the contrary, recent studies have showed that hypoxia could increase the ATF4 expression in tumor cells to promote macrophage recruitment and differentiation via secretion of M-CSF.²³ In line with previous studies,¹ the expression of M-CSF was markedly increased in OKC epithelium when compared with that in normal OM. Meanwhile, the M-CSF expression was closely correlated with ATF4 in the epithelium of OKC, evidenced by both Spearman's rank test and immunofluorescence co-expression. In addition, we found the infiltration of M2-polarized macrophages in OKC stroma was positively correlated with the expression of HIF-1 α , ATF4, and M-CSF in OKC epithelium. What's more, our *in vitro* studies using HIOECs indicated that both of ATF4 and M-CSF expressions were greatly enhanced under hypoxic condition. These results suggest that hypoxia may enhance the expression of M-CSF by activating ATF4 in the epithelium cells of OKC and promote the infiltration of M2-polarized macrophages in the stroma.

Regarding bone resorption in OKC, previous studies have showed that ATF4 could regulate the expression of RANKL, one key factor promoting osteoclastogenesis, to promote the bone destruction.^{10,27} Nevertheless, there was no evidence that ATF4 was associated with RANKL in the OKC epithelium in our present study. RANKL-mediated bone resorption might not be required for the function of ATF4 in the development of OKC. To our interests, M-CSF could bind to its receptor (CSF1R) to contribute to the production of osteoclast progenitors. Meanwhile, M-CSF also activates osteoclasts differentiation and bone resorption in diseases through activating the PI3K/AKT signaling pathway.²⁸ Therefore, ATF4 may also promote the development of OKC by enhancing the bone resorption in OKC, dependent on M-CSF.

However, in our present study, only HIOECs were used for the mechanism investigation *in vitro*. In fact, the best model for OKC-related studies is primary OKC epithelial cells (OKCECs). Unfortunately, the growth of primary OKCECs was very slow, and easily senescent after passage. Currently, the knowledge gained about epithelial cells of OKC is also generated by studies using HIOECs to some extent, as HIOECs are well-established cell models with immortalized proliferation and cellular and molecular stabilities and the source material is readily available. For instance, a study used HIOECs to investigate the crucial role of interaction between epithelial cells and fibroblasts in the bone destruction of OKC.² On the contrary, one research from our group also used HIOECs to study the influence of cell-derived microparticles from the cyst fluids of OKC on the proliferation of epithelial cells in OKC.²⁹ However, OKCECs have been frequently found to be related to some gene mutations, including oncogenic PTCH, L-MYC, CMN, and VHL,³⁰ which indicated that OKCECs are different from HIOECs in the genetic background. Therefore, although our data *in vitro* implicated the role of hypoxia on the expressions of ATF4 and M-CSF in epithelial cells, studies using OKCECs are still needed to strengthen the *in vitro* findings of this study in the future. In conclusion, the present study showed the accumulation of ATF4 in the epithelium of OKC, and its potential association with M2-polarized macrophages infiltration and angiogenesis. Besides, this regulatory network, which involves ATF4 activation and ATF4-associated M-CSF upregulation, could be one of the pathophysiological mechanisms how OKC epithelium cells make response to hypoxia stress. In addition, our research also suggested the interaction between OKC epithelial cells and stromal cells (M2-polarized macrophages) occurred in the pathogenesis of OKC under the regulation of ATF4 in response to hypoxia. Although the

precious mechanisms in this regulatory network remain to be clarified, the ATF4-centered regulation network possesses great value for elucidation of the pathogenesis and treatment of OKC.

Competing Interests

The author(s) declared no potential conflicts of interest with respect to the research, authorship, and/or publication of this article.

Author Contributions

W-QZ and J-HZ conceived and designed the experiments. W-QZ and Z-ZL performed the experiments and analyzed the data. H-J, Y-PZ, and H-TW helped with the analysis of data with constructive discussions. Y-C helped with the collection of clinical samples. Z-ZL wrote and prepared the article. W-QZ and J-HZ critically read and revised the article. All authors have read and approved the final article.

Funding

The author(s) disclosed receipt of the following financial support for the research, authorship, and/or publication of this article: Funding for this research was provided by the grants from Natural Science Foundation of China (81800994) to Dr W.-Q.Z., and Natural Science Foundation of China (81671008) to Prof. J.-H. Z.

Literature Cited

- Zhong WQ, Chen G, Zhang W, Xiong XP, Zhao Y, Liu B, Zhao YF. M2-polarized macrophages in keratocystic odontogenic tumor: relation to tumor angiogenesis. *Sci Rep.* 2015;5:15586.
- Wang HC, Jiang WP, Sima ZH, Li TJ. Fibroblasts isolated from a keratocystic odontogenic tumor promote osteoclastogenesis in vitro via interaction with epithelial cells. *Oral Dis.* 2015;21(2):170–7.
- Zhong WQ, Chen G, Zhang W, Xiong XP, Ren JG, Zhao Y, Liu B, Zhao YF. Down-regulation of connexin43 and connexin32 in keratocystic odontogenic tumours: potential association with clinical features. *Histopathology.* 2015;66(6):798–807.
- Thompson L. World Health Organization classification of tumours: pathology and genetics of head and neck tumours. *Ear Nose Throat J.* 2006;85(2):74.
- Gonzalez-Gonzalez A, Munoz-Muela E, Marchal JA, Cara FE, Molina MP, Cruz-Lozano M, Jimenez G, Verma A, Ramirez A, Qian W, Chen W, Kozielski AJ, Elemento O, Martin-Salvago MD, Luque RJ, Rosa-Garrido C, Landeira D, Quintana-Romero M, Rosato RR, Garcia MA, Ramirez-Tortosa CL, Kim H, Rodriguez-Aguayo C, Lopez-Berestein G, Sood AK, Lorente JA, Sanchez-Rovira P, Chang JC, Granados-Principal S. Activating transcription factor 4 modulates TGF β -induced aggressiveness in triple-negative breast cancer via SMAD2/3/4 and mTORC2 signaling. *Clin Cancer Res.* 2018;24(22):5697–709.
- Lai DW, Lin KH, Sheu WH, Lee MR, Chen CY, Lee WJ, Hung YW, Shen CC, Chung TJ, Liu SH, Sheu ML. TPL2 (Therapeutic Targeting Tumor Progression Locus-2)/ATF4 (Activating Transcription Factor-4)/SDF1 α (Chemokine Stromal Cell-Derived Factor- α) axis suppresses diabetic retinopathy. *Circ Res.* 2017;121(6):e37–52.
- Jin J, Zhao L, Zou W, Shen W, Zhang H, He Q. Activation of cyclooxygenase-2 by ATF4 during endoplasmic reticulum stress regulates kidney podocyte autophagy induced by lupus nephritis. *Cell Physiol Biochem.* 2018;48(2):753–64.
- Galehdar Z, Swan P, Fuerth B, Callaghan SM, Park DS, Cregan SP. Neuronal apoptosis induced by endoplasmic reticulum stress is regulated by ATF4-CHOP-mediated induction of the Bcl-2 homology 3-only member PUMA. *J Neurosci.* 2010;30(50):16938–48.
- Sielska M, Przanowski P, Wylot B, Gabrusiewicz K, Maleszewska M, Kijewska M, Zawadzka M, Kucharska J, Vinnakota K, Kettenmann H, Kotulska K, Grajkowska W, Kaminska B. Distinct roles of CSF family cytokines in macrophage infiltration and activation in glioma progression and injury response. *J Pathol.* 2013;230(3):310–21.
- Tsushima H, Okazaki K, Ishihara K, Ushijima T, Iwamoto Y. CCAAT/enhancer-binding protein β promotes receptor activator of nuclear factor-kappa-B ligand (RANKL) expression and osteoclast formation in the synovium in rheumatoid arthritis. *Arthritis Res Ther.* 2015;17:31.
- Nagelkerke A, Bussink J, Mujcic H, Wouters BG, Lehmann S, Sweep FC, Span PN. Hypoxia stimulates migration of breast cancer cells via the PERK/ATF4/LAMP3-arm of the unfolded protein response. *Breast Cancer Res.* 2013;15(1):R2.
- Notte A, Rebutti M, Fransolet M, Roegiers E, Genin M, Tellier C, Watillon K, Fattaccioli A, Arnould T, Michiels C. Taxol-induced unfolded protein response activation in breast cancer cells exposed to hypoxia: ATF4 activation regulates autophagy and inhibits apoptosis. *Int J Biochem Cell Biol.* 2015;62:1–14.
- Notte A, Ninane N, Arnould T, Michiels C. Hypoxia counteracts taxol-induced apoptosis in MDA-MB-231 breast cancer cells: role of autophagy and JNK activation. *Cell Death Dis.* 2013;4:e638.
- Mujcic H, Nagelkerke A, Rouschop KM, Chung S, Chaudary N, Span PN, Clarke B, Milosevic M, Sykes J, Hill RP, Koritzinsky M, Wouters BG. Hypoxic activation of the PERK/eIF2 α arm of the unfolded protein response promotes metastasis through induction of LAMP3. *Clin Cancer Res.* 2013;19(22):6126–37.
- Harris AL. Hypoxia—a key regulatory factor in tumour growth. *Nat Rev Cancer.* 2002;2(1):38–47.
- Miyauchi Y, Sato Y, Kobayashi T, Yoshida S, Mori T, Kanagawa H, Katsuyama E, Fujie A, Hao W, Miyamoto K, Tando T, Morioka H, Matsumoto M, Chambon P, Johnson RS, Kato S, Toyama Y, Miyamoto T. HIF1 α is required for osteoclast activation by estrogen deficiency in postmenopausal osteoporosis. *Proc Natl Acad Sci U S A.* 2013;110(41):16568–73.

17. Giatromanolaki A, Sivridis E, Maltezos E, Athanassou N, Papazoglou D, Gatter KC, Harris AL, Koukourakis MI. Upregulated hypoxia inducible factor-1 α and -2 α pathway in rheumatoid arthritis and osteoarthritis. *Arthritis Res Ther*. 2003;5(4):R193–201.
18. Li W, Li Y, Guan S, Fan J, Cheng CF, Bright AM, Chinn C, Chen M, Woodley DT. Extracellular heat shock protein-90 α : linking hypoxia to skin cell motility and wound healing. *EMBO J*. 2007;26(5):1221–33.
19. da Costa NM, Fialho AD, Proietti CC, da Silva Kataoka MS, Jaeger RG, de Alves-Junior SM, de Jesus Viana Pinheiro J. Role of hypoxia-related proteins in invasion of ameloblastoma cells: crosstalk between NOTCH1, hypoxia-inducible factor 1 α , a disintegrin and metalloproteinase 12, and heparin-binding epidermal growth factor. *Histopathology*. 2016;69(1):99–106.
20. da Costa NMM, de Siqueira AS, Ribeiro ALR, da Silva Kataoka MS, Jaeger RG, de Alves-Junior SM, Smith AM, de Jesus Viana Pinheiro J. Role of HIF-1 α and CASPASE-3 in cystogenesis of odontogenic cysts and tumors. *Clin Oral Investig*. 2018;22(1):141–9.
21. Aras S, Zaidi MR. TAMEless traitors: macrophages in cancer progression and metastasis. *Br J Cancer*. 2017;117(11):1583–91.
22. Pollard JW. Trophic macrophages in development and disease. *Nat Rev Immunol*. 2009;9(4):259–70.
23. Lewis C, Murdoch C. Macrophage responses to hypoxia: implications for tumor progression and anti-cancer therapies. *Am J Pathol*. 2005;167(3):627–35.
24. Chen G, Zhang W, Li YP, Ren JG, Xu N, Liu H, Wang FQ, Sun ZJ, Jia J, Zhao YF. Hypoxia-induced autophagy in endothelial cells: a double-edged sword in the progression of infantile haemangioma? *Cardiovasc Res*. 2013;98(3):437–48.
25. Li RF, Chen G, Zhao Y, Zhao YF, Liu B. Increased expression of autophagy-related proteins in keratocystic odontogenic tumours: its possible association with growth potential. *Br J Oral Maxillofac Surg*. 2014;52(6):551–6.
26. Azaripour A, Lagerweij T, Scharfbillig C, Jadczyk AE, Swaan BV, Molenaar M, Waal RV, Kielbassa K, Tigchelaar W, Picavet DI, Jonker A, Hendriks EML, Hira VVV, Khurshed M, Noorden C. Three-dimensional histochemistry and imaging of human gingiva. *Sci Rep*. 2018;8(1):1647.
27. Oka S, Kubota Y, Yamashiro T, Ogata S, Ninomiya T, Ito S, Shirasuna K. Effects of positive pressure in odontogenic keratocysts. *J Dent Res*. 2005;84(10):913–8.
28. Boyle WJ, Simonet WS, Lacey DL. Osteoclast differentiation and activation. *Nature*. 2003;423(6937):337–42.
29. Man QW, Zhong WQ, Ren JG, Liu JY, Zheng YY, Li RF, Nyimi BF, Chen G, Zhao YF, Liu B. Increased level of cell-derived microparticles in the cyst fluids of odontogenic keratocysts. *Int J Oncol*. 2018;52(6):1863–74.
30. Agaram NP, Collins BM, Barnes L, Lomago D, Aldeeb D, Swalsky P, Finkelstein S, Hunt JL. Molecular analysis to demonstrate that odontogenic keratocysts are neoplastic. *Arch Pathol Lab Med*. 2004;128(3):313–7.